REPORT: 2016 SCEC Proposal

Rheological Mixing Laws for Application to the Community Rheology Model

PIs – Greg Hirth (Brown University) and Mark Behn (WHOI)

1. Summary, Motivation and Background

We propose to initiate development of a catalogue of rheological flow laws and construct quantitative tools to calculate effective viscosities of crustal rocks appropriate for application in the nascent Community Rheological Model (CRM). Over the last few years, there has been a growing appreciation for how the rheology of the lithosphere is important for several SCEC goals linked to the Community Stress Model (CSM), Community Geodetic Model (CGM), and the SDOT group's goals of constraining the loading of faults at the time scales much greater than an earthquake cycle.

Our goal is to start preparing the database of pertinent mineral and rock flow laws, as well as rheological mixing laws which are necessary to calculate effective viscosities for crustal rocks. In anticipation of preparatory efforts to construct a Community Thermal Model (CTM), as well as efforts to constrain pertinent rock types based on relationships between seismic velocity (Vp, Vs, Vp/Vs) and rock composition, we describe here the efficacy of calculating rock viscosity based on composition and highlight where important assumptions about rheology need to be considered. The products of our analyses will be tractable macros and catalogues that should be easily incorporated into a CRM as the project matures – in collaboration with the other SCEC scientists leading efforts to develop the CTM, seismic imaging and geodynamic modelling. These efforts will also provide a "rheological backbone" onto which additional processes can be studied, such as grain size evolution, transient creep and the evolution of macroscopic shear zone structure – all of which are important for understanding processes responsible for lithospheric-scale strain localization, the interpretation of post-seismic creep, and understanding earthquake rupture dynamics near the brittle-plastic transition.

2. Methodology for Calculating Effective Crustal Viscosity

Here we illustrate results from our last year of SCEC-funded research focused on estimating effective crustal viscosity by integrating constraints from seismic velocity and multi-phase mixing theory. Over the last decade, extensive data bases of crustal rock compositions have been compiled [*Hacker et al.*, 2015]. Previous work has quantified the relationship between seismic velocity and crustal composition [e.g., *Behn and Kelemen*, 2003]. Here we illustrate the additional relationship linking seismic velocity to viscosity for a given strain rate, pressure, and temperature.

In Figure 1, we show calculations of V_P and V_S for a broad range of rock compositions color-coded as a function of the calculated viscosity. For each bulk composition, we use thermodynamic phase equilibria calculation (Perple X, *Connolly*, 2009) to estimate stable mineral assemblages under pressure and temperature (P-T) conditions appropriate for the lower crust. The seismic velocities are then calculated within Perple X using the modeled mineral assemblages and the densities and elastic constants of the minerals at the appropriate conditions.

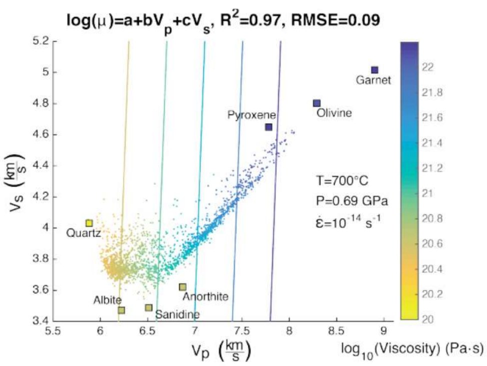

Figure 1: Viscosity calculated as a function of *Vp* and *Vs* for 3500 characteristic crustal rock compositions. For each composition the mineral mode is estimated using Perple_X at 700°C and 0.69 GPa. Mineral modes are then used to estimate seismic velocity and viscosity based on mixing laws. Major minerals are also plotted. Solid lines denote lines of constant viscosity based on a linear fit of viscosity to *Vp* and *Vs* following the relation $\log(\eta)=a+bVp+cVs$.

To calculate the aggregate viscosity from the equilibrium mineral assemblages, we employ the mixing model of *Huet et al.* [2014]. This method assumes a large enough scale that the rock can be considered homogeneous and isotropic. Based on our phase equilibria calculations, we consider four major crustal minerals: quartz, feldspar (plag + alkali feldspar), pyroxene (opx + cpx), and garnet; together, these phases typically make up >90% of the crust by volume in our calculations. Flow laws for quartz, feldspar, and pyroxene are taken from *Hirth et al.* [2001], *Rybacki et al.* [2006], and *Dimanov & Dresen* [2005], and include a water fugacity term in all flow laws (Figure 2). The applicability of most of these flow laws (i.e., quartzite, plagioclase, pyroxenite) at geologic strain rates has been tested through a combination of microstructural analyses and thermobarometry/chronology of naturally deformed rocks from well-preserved structural environments under both dry and wet rheological conditions [e.g., *Mehl and Hirth*, 2008; *Behr and Platt*, 2011, *Getsinger et al.*, 2013]. *Huet et al.* [2014] demonstrate that the continuum mixing laws provide a good fit to experimental data on two-phase aggregates.

Our previous work [*Shinevar et al.*, 2015] illustrates that the viscosities calculated for average lower crustal compositions ranging from basaltic to andesitic [e.g., *Rudnick & Gao*, 2003; *Hacker et al.*, 2011] agree well independent estimates of lower crustal viscosity in actively deforming regions based on geodetic studies [e.g., *Thatcher & Pollitz*, 2008] (Figure 3). These calculations indicate that under the same P-T and strain-rate, andesitic lower crust has a viscosity that is approximately 10 to 30 times lower than a basaltic lower crust, illustrating the strong influence of rock composition on predicted rheology. Geodetic viscosity estimates range from 10^{19}–10^{21} Pa·s for tectonically active regions with estimated strain rates between 10^{-13}–10^{-14} s^{-1} [*Thatcher & Pollitz*, 2008] and average heat flow of ~80 mW/m^2 [*Lee & Uyeda*, 1965; *Pollack &Chapman*, 1977] (grey boxes in **Fig. 3**). More recent studies give similar estimates, with slightly lower crustal viscosities ranging from 3.1 x 10^{18}–3.1 x 10^{20} [*Hammond et al.*, 2009; *Pollitz & Thatcher*, 2010;

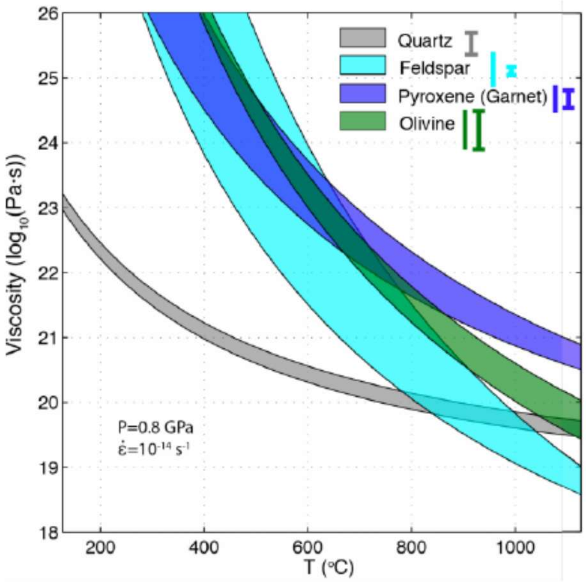

Figure 2: Viscosity as a function of temperature for major crust forming minerals. Upper and lower viscosity bounds are calculated under dry and wet conditions, respectively. Specifically, bounds are calculated for quartz (a_{H2O} = 0.1, a_{H2O} = 1). From *Shinevar et al*. (2015)

Chang et al., 2013]. In all of the geodetic studies, the lower crust is modeled as a single layer with constant viscosity, and thus, we take these values as an estimate of the average viscosity over the lower crust (15-30km; grey boxes in Fig. 3). The estimates from the postseismic relaxation studies must be considered lower bounds, because of the short time span (<40 years) over which relaxation has been analyzed. Nonetheless, analyses of paleolake shorelines in Tibet provide lower bounds for long-term lower crustal viscosities similarto those estimated from postseismic relaxation in the same region [*England et al*., 2013; *Shi et al*., 2015].

Returning to Figure 1, we see a strong correlation between the seismic velocity and viscosity at 700ºC, presaging the efficacy of using seismic velocity from the CVM to constrain lower crust viscosity in Southern California. Fitting these data with a relationship of the form $\log(\eta) = a + bV_p + cV_s$ results in an $R^2 = 0.97$ (Figure 1).

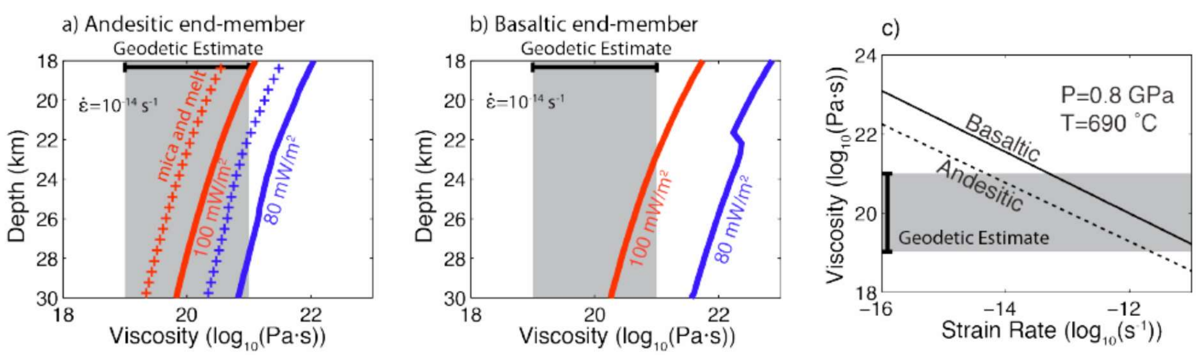

Figure 3: Viscosity calculated as a function of depth for the (a) andesitic and (b) basaltic end-member compositions along 80 mW/m^2 (blue) and 100 mW/m^2 (red) geotherms. The crossed lines in (a) denote the estimated factor of two viscosity drop due to the presence of mica or melt (100mW/m^2) in the modal composition. Calculations assume a background strain rate of 10^{-14} s^{-1}. Grey region denotes independent viscosity constraints from post-seismic relaxation and isostatic rebound [Thatcher & Pollitz, 2008]. (c) Aggregate viscosity as a function of strain rate for both end-member compositions at ~30 km depth on an 80 mW/m^2 geotherm (690ºC and 0.8 GPa).

Linking viscosity calculations to the Community Velocity Model.

Using our relationship between seismic velocity and viscosity, we infer the viscosity structure of Southern California based on the CVM (Figure 4). Our initial results assumed a constant crustal temperature of 700ºC at 7 kbar (~25 km depth). This approach likely over-estimates the effect of composition on viscosity because it maps all of the velocity perturbations into variations in viscosity due to changes in crustal lithology. Thus, our next goal is to follow a similar approach but using a more realistic thermal structure that takes into account lateral variability. To do so, we can utilize regional heat flow data (Figure 4d) and available constraints on crustal heat production – data that are being compiled as part of the CTM. Further, we need to incorporate a more accurate model for crustal thickness. For example, the region near the Salton Trough characterized by both high heat flux (Figure 4d) and high viscosity (Figure 4c), could represent an area with anomalously thin crust where the Moho is located shallower than 25 km depth [e.g., *Parsons and McCarthy*, 1996]. In this case our seismic velocity to viscosity relationship for crustal rocks cannot be applied directly to the seismic data.

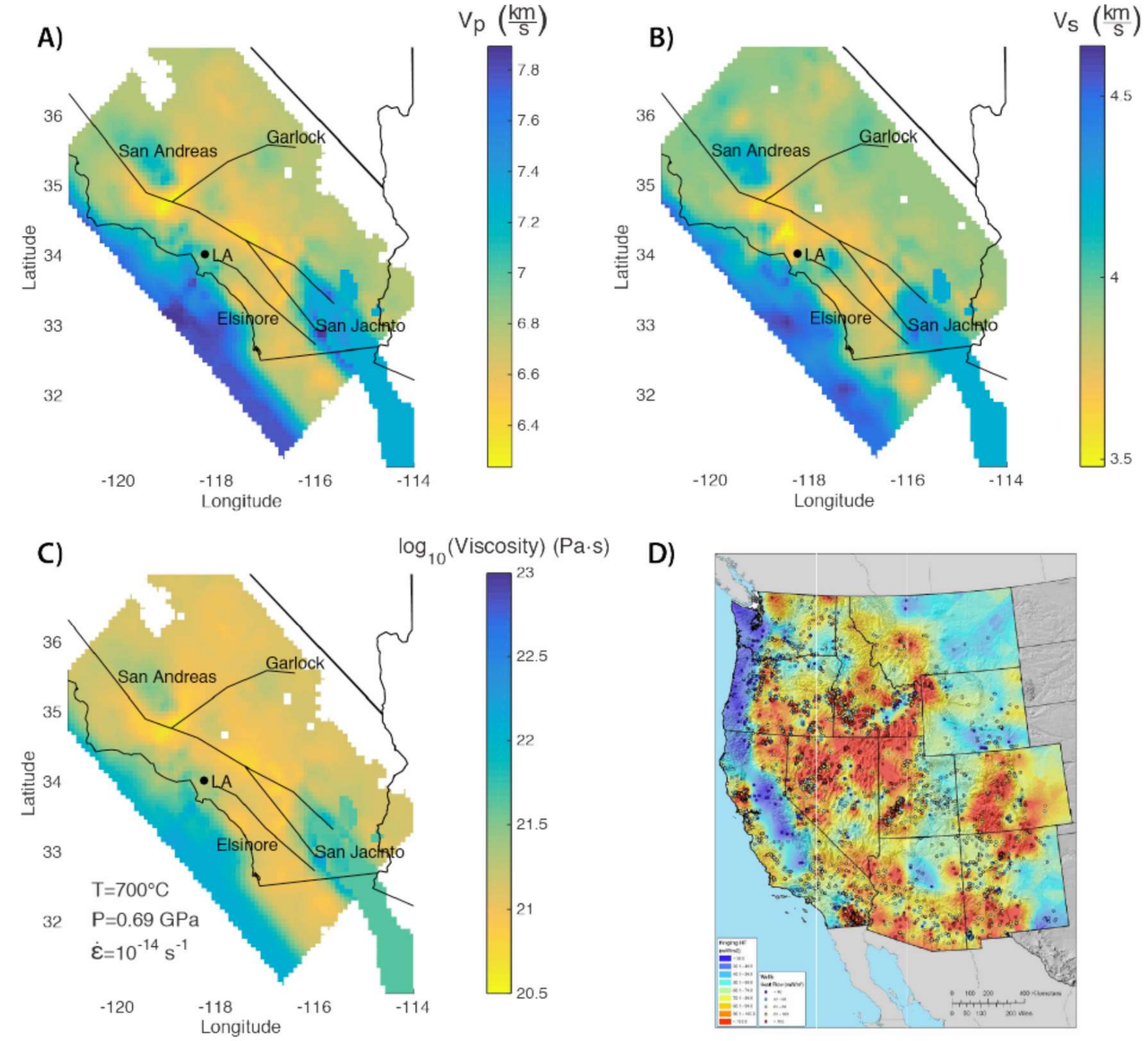

Figure 4: Example calculation of crustal viscosity based on the Community Velocity Model (CVM). (A) Vp and (B) Vs from the CVM at a depth of 25 km. (C) Viscosity interpolated based on the relationship shown in **Figure 1** assuming a background mantle strain rate of 10^{-14} s^{-1}. (D) Heat flow map of western North America from Williams & DeAngelo [2011]. Note the region of high heat flux and high viscosity near the Salton Trough.

Inferring Crustal Viscosity Structure from the CVM

Shinevar, Behn, Hirth & Jagoutz

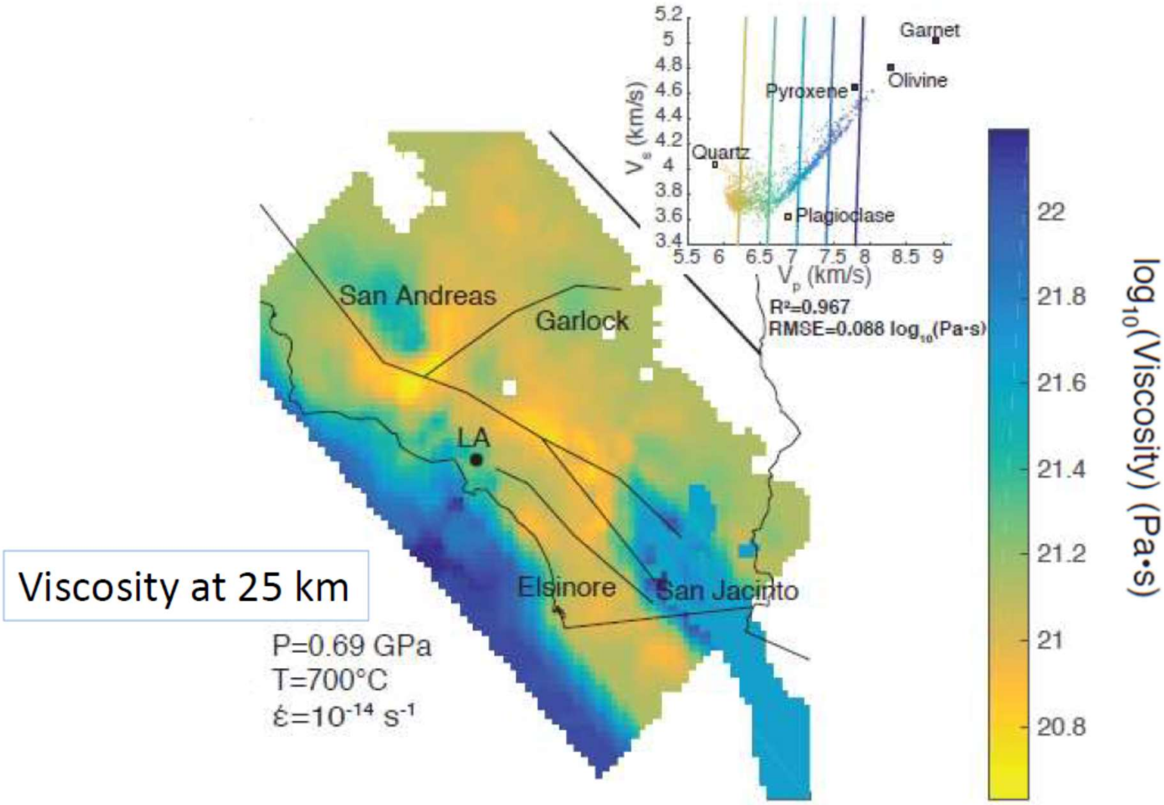

EXEMPLARY FIGURE: We use seismic velocity (P and S wave) from the SCEC CVM to constrain lower crustal viscosity. Our analysis follows a three-step approach. First, we use the Gibbs free energy minimization routine Perple_X to calculate equilibrium mineral assemblages and seismic velocities for a global compilation of lower crustal rocks (Hacker et al. *AREPS*, 2015) at various pressures and temperatures. Second, we use the Huet et al. (*JGR*, 2014) mixing model and single-phase flow laws for major crust-forming minerals to calculate bulk viscosity for the predicted equilibrium mineral assemblages. Finally, we linearly fit the viscosity calculations to the seismic velocity calculations. This method provides a strong (R^2>0.9) fit in the alpha-quartz regime. Our figure shows a viscosity map for 25km depth assuming T=700°C and $\dot{\varepsilon}=10^{-14}$ s^{-1} as well as the viscosity-velocity data shown in the upper right hand corner. High viscosity in the Salton Trough is measuring mantle, rather than crustal behavior, owing to shallow Moho. The colored lines are the estimated fit. Our results are in agreement with regional geodetic estimates from Freed et al. (*GRL*, 2007).

4. References

Behn, M. D., M. S. Boettcher, & G. Hirth (2007). Thermal structure of oceanic transform faults. *Geology*, 35(4), 307-310.

Behn, M.D., G. Hirth and J.R. Elsenbeck II (2009), Implications of grain-size evolution on the seismic structure of the oceanic upper mantle, *Earth Planet. Sci. Lett.*, 282, 178-189, doi:10.1016/j.epsl.2009.03.014.

Behr, W.M., Platt, J.P. (2011), A naturally constrained stress profile through the middle crust in an extensional terrane, *Earth and Planetary Science Letters*, 303, 181-192.

Chang, W. L., R. B. Smith, & C. M. Puskas (2013). Effects of lithospheric viscoelastic relaxation on the contemporary deformation following the 1959 Mw 7.3 Hebgen Lake, Montana, earthquake and other areas of the intermountain seismic belt. *Geochemistry, Geophysics, Geosystems*, 14(1), 1-17.

Connolly, JAD (2009) The geodynamic equation of state: what and how. *Geochemistry, Geophysics, Geosystems* 10:Q10014 DOI:10.1029/2009GC002540.

Dimanov, A. & G. Dresen (2005). Rheology of synthetic anorthite-diopside aggregates: Implications for ductile shear zones. *Journal of Geophysical Research: Solid Earth* (1978–2012), 110(B7).

England, P. C., R. T. Walker, B. Fu, and M. A. Floyd (2013), A bound on the viscosity of the Tibetan crust from the horizontality of palaeolake shorelines, *Earth Planet. Sci. Lett.*, **375**, 44–56.

Getsinger, A.J., G. Hirth, H. Stunitz, and E.T. Goergen, The influence of water on rheology and strain localization in the lower continental crust, *G-cubed*, 14, 2247-2264, DOI: 10.1002/ggge.20148, 2013.

Getsinger, A., and G. Hirth, Amphibole fabric formation during diffusion creep and the rheology of shear zones, *Geology*, 42, 535-538, doi:10.1130/G35327.1, 2014.

Hacker, B. R., P. B. Kelemen, & M. D. Behn (2011). Differentiation of the continental crust by relamination. *Earth and Planetary Science Letters*, 307(3), 501-516.

Hacker, B.R., & J. M. Christie, (1990), Brittle/ductile and plastic/cataclastic transitions in experimentally deformed and metamorphosed amphibolite: *Geophysical Monograph*, v.56, p. 127–147

Hammond, W. C., C. Kreemer, & G. Blewitt (2009). Geodetic constraints on contemporary deformation in the northern Walker Lane: 3. Central Nevada seismic belt postseismic relaxation. *Geological Society of America Special Papers*, 447, 33-54.

Hirth, G., C. Teyssier, & J. W. Dunlap (2001). An evaluation of quartzite flow laws based on comparisons between experimentally and naturally deformed rocks. *International Journal of Earth Sciences*, 90(1), 77-87.

Huet, B., P. Yamato, & B. Grasemann (2014). The Minimized Power Geometric model: An analytical mixing model for calculating polyphase rock viscosities consistent with experimental data. *Journal of Geophysical Research: Solid Earth*, 119(4), 3897-3924.

Ji, S., & J. Martignole (1994). Ductility of garnet as an indicator of extremely high temperature deformation. *Journal of Structural Geology*, 16(7), 985-996.

Kidder, S., G. Hirth, J.-P. Avouac, and W. Behr, The influence of stress history on the grain size and microstructure of experimentally deformed quartzite, *J. Struct. Geol.*, submitted.

Kronenberg, A. K., S. H. Kirby, & J. Pinkston (1990). Basal slip and mechanical anisotropy of biotite. *Journal of Geophysical Research: Solid Earth* (1978–2012), 95(B12), 19257-19278.

Lee, W. H., & S. Uyeda (1965). Review of heat flow data. I*n Terrestrial heat flow* (Vol. 8, pp. 87-190). American Geophysical Union Washington, DC.

Mehl, L., and G. Hirth (2008), Plagioclase preferred orientation in layered mylonites: Evaluation of flow laws for the lower crust, *J. Geophys. Res.*, **113**, B05202, doi:10.1029/2007JB005075.

Parsons, T., and J. McCarthy, Crustal and upper mantle velocity structure of the Salton Trough, southeast California, *Tectonics*, 15, 456-471, 1996.

Platt, J. P., and W. M. Behr (2011)."Grainsize evolution in ductile shear zones: Implications for strain localization and the strength of the lithosphere. *Journal of Structural Geology* 33.4, 537-550.

Pollitz, F. F., & W. Thatcher (2010). On the resolution of shallow mantle viscosity structure using postearthquake relaxation data: Application to the 1999 Hector Mine, California, earthquake. *Journal of Geophysical Research: Solid Earth* (1978–2012), 115(B10).

Pollack, H. N., & D.S. Chapman (1977). On the regional variation of heat flow, geotherms, and lithospheric thickness. *Tectonophysics*, 38(3), 279-296.

Rudnick, R. L. & S. Gao (2003). Composition of the continental crust. *Treatise on Geochemistry*, 3, 1-64.

Rybacki, E., M. Gottschalk, R. Wirth, & G. Dresen (2006). Influence of water fugacity and activation volume on the flow properties of fine-grained anorthite aggregates. *Journal of Geophysical Research: Solid Earth* (1978–2012), 111(B3).

Shi, X., E. Kirby, K. P. Furlong, K. Meng, R. Robinson, and E. Wang (2015), Crustal strength in central Tibet determined from Holocene shoreline deflection around Siling Co, *Earth Planet. Sci. Lett.*, **423**, 145–154.

Shinevar, W.J., M.D. Behn, & G. Hirth (2015). Compositional dependence of lower crustal viscosity, *Geophys. Res. Lett.*, 42, 8333-8340, doi:10.1002/2015GL065459.

Thatcher, W. & F. F. Pollitz (2008). Temporal evolution of continental lithospheric strength in actively deforming regions. *GSA Today*, 18(4/5), 4.

Tokle, L., H. Stunitz, & G. Hirth (2013). The effect of muscovite on the fabric evolution of quartz under general shear. *In AGU Fall Meeting Abstracts* (Vol. 1, p. 2559).

Tullis, J., & Wenk, H. R. (1994). Effect of muscovite on the strength and lattice preferred orientations of experimentally deformed quartz aggregates. *Materials Science and Engineering: A*, 175(1), 209-220.